Journal of the Physical Society of Japan **80** (2011) 073702 LETTERS
DOI: 10.1143/JPSJ.80.073702

Quadrupole Effects of Layered Iron Pnictide Superconductor $Ba(Fe_{0.9}Co_{0.1})_2As_2$

Terutaka GOTO[1,2]*, Ryosuke KURIHARA[1], Koji ARAKI[1], Keisuke MITSUMOTO[1], Mitsuhiro AKATSU[1], Yuichi NEMOTO[1,2], Shunichi TATEMATSU[3], and Masatoshi SATO[2,3,4]

[1]*Graduate School of Science and Technology, Niigata University, Niigata 950-2181, Japan*
[2]*JST, Transformative Research-Project on Iron Pnictides (TRIP), Chiyoda, Tokyo 102-0075, Japan*
[3]*Department of Physics, Nagoya University, Nagoya 464-8602, Japan*
[4]*Toyota Physical and Chemical Research Institute, Nagakute, Aichi 480-1192, Japan*

(Received April 13, 2011; accepted May 9, 2011; published online June 27, 2011)

Elastic constant measurements on iron pnictide $Ba(Fe_{0.9}Co_{0.1})_2As_2$ with an optimal superconducting transition temperature of $T_{SC} = 23$ K have been performed by the ultrasonic pulse echo method. The shear elastic constant of C_{66} associated with elastic strain ε_{xy} reveals considerable softening of 21% below 300 K down to T_{SC} and becomes increasing in the superconducting phase below T_{SC}, while other shear elastic constants of $(C_{11} - C_{12})/2$ and C_{44} show no sign of softening below 80 K down to 4.2 K. The electric quadrupole $O_{v'}$ existing in the degenerate $d_{y'z}$ and $d_{zx'}$ bands participates in the superconductivity of the present iron pnictide system.

KEYWORDS: layered iron pnictide, superconductor, $Ba(Fe_{0.9}Co_{0.1})_2As_2$, elastic softening

The discovery of the superconductor $LaFeAs(O_{1-x}F_x)$ with a high transition temperature of $T_{SC} = 26$ K by Hosono's group triggered thousands of research works pursuing FeAs-based superconductors with various chemical composites and different structures.[1)] Five crystal structures with a common iron-based layer structure are now known.[2)] The high transition temperatures of up to 55 K and high critical magnetic fields beyond 50 T have already been realized.[3,4)] Among these FeAs-based crystals, the tetragonal compound of $Ba(Fe_{1-x}Co_x)_2As_2$, in particular, has received much attention, because large single crystals are available for the investigation of physical properties depending on crystal anisotropy.[5)]

The end-material $BaFe_2As_2$ exhibits a simultaneous transition of structural transition from a tetragonal $TrCr_2Si_2$-type structure of space group D_{4h}^{17} $(I4/mmm)$ to an orthorhombic one of D_{2h}^{23} $(Fmmm)$ at $T_s = 140$ K and of a stripe-type antiferromagnetic order at $T_N = T_s$.[6,7)] The electron doping upon the substitution of Fe^{2+} with $3d^6$ orbitals by Co^{2+} with $3d^7$ orbitals in $Ba(Fe_{1-x}Co_x)_2As_2$ reduces both the structural transition temperature of T_s and the antiferromagnetic one of T_N.[8)] The superconductivity emerges in the systems above $x = 0.03$ at the temperatures of T_{SC} below the structural point T_s and the antiferromagnetic one T_N. The quantum critical point, x_{QCP}, where both structural and antiferromagnetic phases die out, exists in the proximity of $x = 0.07$. The optimum superconducting temperatures of $T_{SC} = 23$ K are achieved with $x = 0.10$, which is a slightly excess of the quantum critical concentration x_{QCP}. The superconductivity vanishes in the highly doped region of $x = 0.17$.

The Fermi surfaces of iron pnictides arise from Fe-3d orbitals and have three hole bands at a Γ-point and two electron bands at an X-point. These bands consist primarily of $d_{y'z}$ and $d_{zx'}$ with Γ_5 under tetragonal symmetry and $d_{x'^2-y'^2}$ with Γ_3.[9)] The increasing of the Fermi level upon electron doping due to the substitution of Fe with Co reduces the three sheets of hole bands around the Γ point in the end-material $BaFe_2As_2$ to two sheets of hole bands in the present $Ba(Fe_{0.9}Co_{0.1})_2As_2$. We adopt the electric quadrupole associated with the degenerate $d_{y'z}$ and $d_{zx'}$ orbital states to describe elastic properties of the compound $Ba(Fe_{1-x}Co_x)_2As_2$. It is noted that the coordinates x' and y' of the quadrupole are oriented to the neighboring Fe–Fe direction, which are rotated 45° with respect to the crystal axes of x and y spanned the neighboring Ba–Ba ions.

The symmetry of superconducting states of iron pnictides has already been argued. The Knight shift in NMR and angle-resolved photoemission spectroscopy experiments suggest an s-wave superconducting order parameter.[10,11)] An antiferromagnetic-fluctuation-mediated sign-reversing s-wave (s_{+-}-wave) state is proposed as a theoretical origin of the superconducting state.[12,13)] The s_{+-}-wave seems to be consistent with most of the experiments.[2)] The superconducting state is considerably robust, however, against the substitution of Fe ions by nonmagnetic impurities.[14,15)] The weak effect on the superconducting transition temperature in the nonmagnetic impurity substitution indicates an s-wave state, which is free from sign reversal (s_{++}-wave). Therefore, the s_{++}-wave state induced by orbital fluctuation is proposed as a plausible pairing state.[16,17)]

Because the electric quadrupole, which is occasionally called the orbital, couples with the elastic strain, the ultrasonic measurements can be a good probe for examining the quadrupole effects of the orbital electronic systems. It has already been reported that the elastic constants in $Ba(Fe_{1-x}Co_x)_2As_2$ reveal softening with decreasing temperature. The resonance ultrasonic spectroscopy of the end material of $x = 0$ and the superconductivity system of $x = 0.08$ by Fernandes *et al.* shows the softening in the shear elastic constant C_{66}.[18)] The ultrasonic pulse echo measurement by Yoshizawa *et al.* reveals the elastic softening in shear elastic constants, including C_{66} in the underdoped systems of $x = 0.037$ and 0.06.[19)] In the present work, we carried out ultrasonic pulse echo measurements on the optimally doped system of $x = 0.10$ to elucidate the interplay of the quadrupole effects in the superconductivity of the system.

Single crystals of the iron pnictide superconductor $Ba(Fe_{0.9}Co_{0.1})_2As_2$ with an optimized superconducting transi-

*E-mail: goto@phys.sc.niigata-u.ac.jp

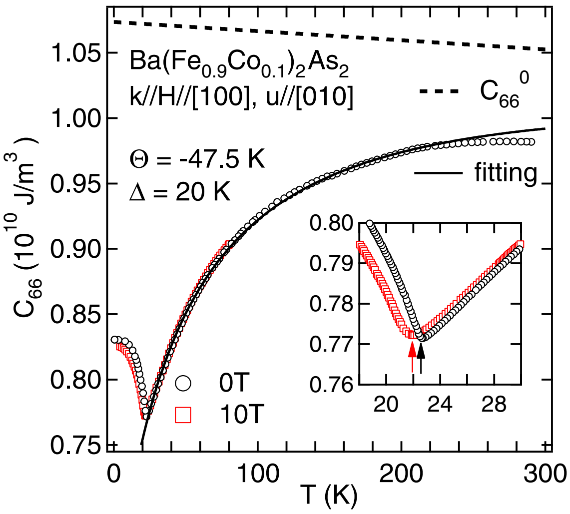

Fig. 1. (Color online) Temperature dependence of shear elastic constant C_{66} of optimally doped iron pnictide $Ba(Fe_{0.9}Co_{0.1})_2As_2$ in zero magnetic field and in magnetic field of 10 T along [100] parallel to propagation direction. The inset shows behavior of C_{66} around superconducting transition temperature $T_{SC} = 23$ K at 0 T and $T_{SC} = 22$ K at 10 T. Arrows indicate the superconducting transition temperature.

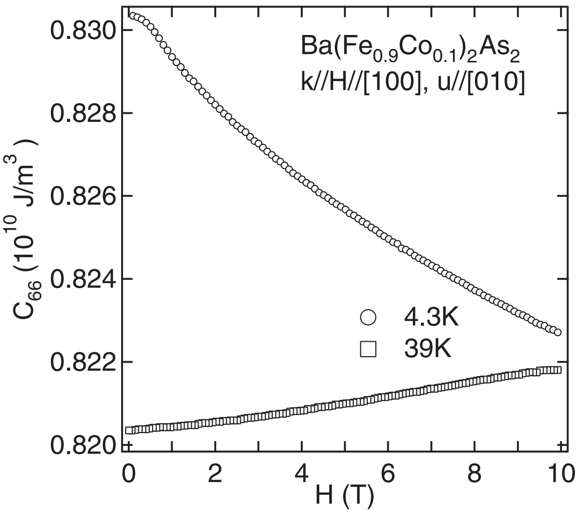

Fig. 2. Field dependence of elastic constant C_{66} at 39 K in normal phase and at 4.3 K in superconducting phase. The magnetic fields were applied along the propagation direction of $\boldsymbol{k} \parallel [100]$ of the C_{66} mode.

tion temperature of $T_{SC} = 23$ K were grown by the Bridgman method. The Laue X-ray photograph was used to determine the axes of the grown crystal. The crystal has a habit with a flat shape of 0.7 mm in thickness along the tetragonal z-axis. We successfully prepared two samples consisting of plane parallel (100) surfaces separated by 1.52 mm and (110) surfaces by 1.50 mm.

The piezoelectric plate of the $LiNbO_3$ 36° Y-cut transducer with 40 µm thickness was employed for the generation and detection of longitudinal ultrasonic waves with frequencies of 75 MHz and the X-cut plate with 40 µm was used for transverse waves with 40 MHz. The ultrasonic velocities v as a function of temperature and applied magnetic field were measured using a home-made apparatus based on a phase-comparison method. The elastic constant is obtained as $C = \rho v^2$ with density $\rho = 6.55\,\mathrm{g{\cdot}cm^{-3}}$ for the present $Ba(Fe_{0.9}Co_{0.1})_2As_2$ with lattice parameters of $a = b = 0.3964$ nm and $c = 1.298$ nm.[20] The ^{3}He-cryostat was employed for low-temperature measurements down to 0.45 K. Magnetic fields of up to 10 T were generated with a superconducting magnet.

The temperature dependence of the shear elastic constant C_{66} of a tetragonal $Ba(Fe_{0.9}Co_{0.1})_2As_2$ crystal is pictured in Fig. 1. The transverse ultrasonic waves of frequencies 40 MHz with propagation vector $\boldsymbol{k} \parallel [100]$ and polarization one $\boldsymbol{u} \parallel [010]$ were employed for the measurements of C_{66} in Fig. 1. This transverse C_{66} mode is associated with the elastic strain ε_{xy} with Γ_3 symmetry. The temperature dependence of C_{66} under zero magnetic field, which is shown by open circles in Fig. 1, reveals marked softening of 21% with decreasing temperature below 300 K down to the superconducting transition of $T_{SC} = 23$ K. An up-turn in C_{66} is observed with further lowering of the temperature in the superconducting phase below T_{SC}. C_{66} shows saturation close to the base temperature of 0.45 K.

In Fig. 1, we also show the temperature dependence in C_{66} of $Ba(Fe_{0.9}Co_{0.1})_2As_2$ under magnetic fields of 10 T applied along the [100] direction, by open squares. As one can see in the inset of Fig. 1, the superconducting transition temperature corresponding to the minimum in C_{66} indicated by arrows is lowered to $T_{SC} = 22$ K in the field of 10 T. C_{66} showing softening in the normal phase above T_{SC} slightly increases with applied magnetic field of 10 T, while C_{66} in the superconducting phase shows a slight reduction in the field of 10 T.

The magnetic field dependence of C_{66} is shown in Fig. 2. The elastic constant C_{66} at 39 K in the normal phase increases 0.3% upon increasing the magnetic field along the [100] direction up to 10 T. At 4.3 K in the superconducting phase, however, the elastic constant C_{66} decreases 1.0% in applied magnetic fields of up to 10 T, in comparison with that in zero field.

The longitudinal elastic constants of C_{11} and C_{33}, and shear ones of $(C_{11} - C_{12})/2$ and C_{44} in $Ba(Fe_{0.9}Co_{0.1})_2As_2$ are shown in Fig. 3. These elastic constants commonly show a monotonic increase with decreasing temperature and small dips around the superconducting transition temperature $T_{SC} = 23$ K. The result for C_{33} in Fig. 3(d) is presented as relative changes of $\Delta C_{33}/C_{33}$, because the short sample length of 0.7 mm along the [001] direction in the present sample causes difficulty in identifying successive echo signals. The normal temperature dependence of C_{11}, C_{33}, $(C_{11} - C_{12})/2$, and C_{44} in Fig. 3 is in contrast to the considerable softening of C_{66} in Fig. 1.

It is worthwhile to consider the symmetry aspect for the present experimental results of the softening in C_{66}. The doubly degenerate $d_{y'z}$ and $d_{zx'}$ orbital states of Fe^{2+} ions written as $|\phi_{y'z}\rangle = -(|1\rangle - |{-1}\rangle)/\sqrt{2}$ and $|\phi_{zx'}\rangle = i(|1\rangle + |{-1}\rangle)/\sqrt{2}$, rule the physical properties of the present system. Here, $|l_z\rangle$ means a ket of angular momentum l_z for 3d-electronic states with $l = 2$. The symmetry product of Γ_5 representation corresponding to the degenerate $d_{y'z}$ and $d_{zx'}$ orbital states is reduced as

$$\Gamma_5 \otimes \Gamma_5 = \Gamma_1 \oplus \Gamma_2(l_z) \oplus \Gamma_3(O_{v'} = l_{x'}^2 - l_{y'}^2) \oplus \Gamma_4(O_{x'y'} = l_{x'}l_{y'} + l_{y'}l_{x'}). \quad (1)$$

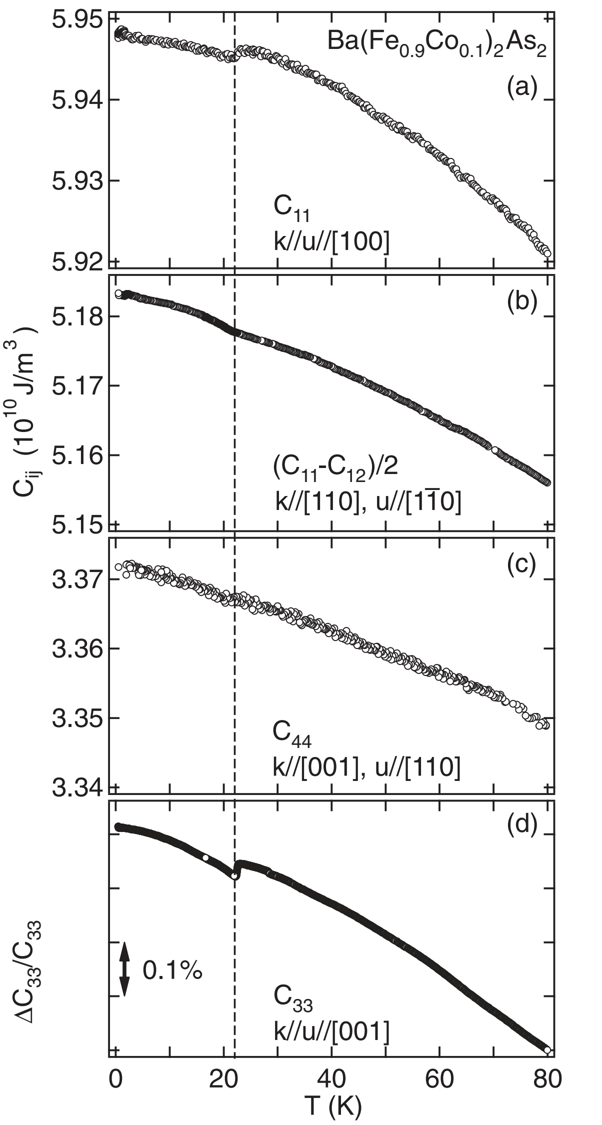

Fig. 3. Temperature dependence in elastic constants C_{11} (a), $(C_{11} - C_{12})/2$ (b), C_{44} (c), and C_{33} (d) of $Ba(Fe_{0.9}Co_{0.1})_2As_2$. The dashed line indicates the superconducting transition temperature $T_{SC} = 23$ K.

It is notable that the electric quadrupoles of $\sigma_x = -O_{x'y'}/3$, $\sigma_z = O_{v'}/3$, and angular momentum of $\sigma_y = -l_z$ satisfy the Pauli commutation relations of $[\sigma_i, \sigma_j] = 2i\varepsilon_{ijk}\sigma_k$. Here, ε_{ijk} is an antisymmetric symbol. This is a common feature of a specially unitary group SU(2). This symmetry analysis promises that the electric quadrupole $O_{v'}$ couples with the elastic strain ε_{xy} of the C_{66} mode. This quadrupole-strain coupling may bring about the softening in C_{66} observed in the present experiments.

The present system consists of the degenerate $d_{y'z}$ and $d_{zx'}$ orbital states that participate in the formation of two-hole Fermi surfaces around the Γ-point and two-electron ones at the X-point. Therefore, the band electrons with finite wave vectors deviating from the Γ- and X-points do not obey symmetry properties of the Fe^{2+} atomic orbitals in the strict meaning. Nevertheless, the elastic softening of C_{66} in Fig. 1 is described in terms of the coupling of the electric quadrupole $O_{v'}$ of the mostly degenerate bands $d_{y'z}$ and $d_{zx'}$ to the elastic strain ε_{xy}. The absence of softening in $(C_{11} - C_{12})/2$ in Fig. 2 indicates that the electric quadrupole of $O_{x'y'}$ plays an irrelevant role in the present system. The role of angular momentum l_z with Γ_2 for the present system is unclear.

The softening of C_{66} in Fig. 1 is described in terms of a strain susceptibility for the 3d-electron bands consisting of the degenerate $d_{y'z}$ and $d_{zx'}$ orbital states, which are lifted, in particular, by the external strain ε_{xy} with the Γ_3 symmetry associated with the transverse ultrasonic C_{66} waves. This coupling is described by a quadrupole-strain interaction Hamiltonian,

$$H_{QS} = -gO_{v'}\varepsilon_{xy}. \tag{2}$$

Here, g is a coupling constant, which is determined from the experiments of softening.

The energy $E_s(\boldsymbol{k})$ of the electrons with wave vector $\boldsymbol{k}$ belonging to branch s is perturbed as a function of the external strain ε_{xy}. Consequently, we obtain the free energy consisting of the system with the energy $E_s(\boldsymbol{k})$ for the band electrons of suffix s with wave vector $\boldsymbol{k}$ and elastic energy of the lattice as[21–23)]

$$F_{el} = nE_F - k_BT\sum_{s,\boldsymbol{k}} \ln\left\{1 + \exp\left[\frac{E_F - E_s(\boldsymbol{k})}{k_BT}\right]\right\}, \tag{3}$$

$$F_{lattice} = \frac{1}{2}C_{66}^0\varepsilon_{xy}^2. \tag{4}$$

Here, n is the number of electrons per unit volume and E_F is the Fermi energy. The second derivative of the free energy with respect to the external strain ε_{xy} leads to the strain susceptibility χ_0 as

$$\begin{aligned}\frac{\partial^2 F_{el}}{\partial\varepsilon_{xy}^2} &= -Dg^2\chi_0 \\ &= \sum_{s,\boldsymbol{k}}\frac{\partial^2 E_s(\boldsymbol{k})}{\partial\varepsilon_{xy}^2}f_{\boldsymbol{k}} - \frac{1}{k_BT}\sum_{s,\boldsymbol{k}} d_{xy}^2(\boldsymbol{k})f_{\boldsymbol{k}}(1-f_{\boldsymbol{k}}) \\ &\quad + \frac{1}{k_BT}\frac{\left|\sum_{s,\boldsymbol{k}} d_{xy}(\boldsymbol{k})f_{\boldsymbol{k}}(1-f_{\boldsymbol{k}})\right|^2}{f_{\boldsymbol{k}}(1-f_{\boldsymbol{k}})}.\end{aligned} \tag{5}$$

Here, D is the density of states at the Fermi level, $d_{xy} = \partial E_s(\boldsymbol{k})/\partial\varepsilon_{xy}$ is the deformation potential, and $f_{\boldsymbol{k}}$ is the Fermi distribution function, respectively. Taking into account the quadrupole interaction g' among the $d_{y'z}$ and $d_{zx'}$ orbital electrons, we obtain the temperature dependence of the elastic constant C_{66} as

$$C_{66} = C_{66}^0 - \frac{Dg^2\chi_0}{1 - g'\chi_0}. \tag{6}$$

The strain susceptibility for one electron of $d_{y'z}$ and $d_{zx'}$ orbitals is governed by the Curie term as $\chi_0 = 1/T$. Therefore, we obtain the temperature dependence of C_{66} as

$$C_{66} = C_{66}^0\left(1 - \frac{\Delta}{T - \Theta}\right). \tag{7}$$

It is noted that eq. (7) is widely used to describe the softening in elastic constants of crystals with degenerate orbital electrons.[21)] The Weiss temperature Θ in eq. (7) represents the coupling energy of the electric quadrupole $O_{v'}$ among the degenerate $d_{y'z}$ and $d_{zx'}$ orbitals. The Jahn–Teller energy $\Delta = Dg^2/C_{66}^0$ is energy gain due to the coupling of the quadrupole $O_{v'}$ via the elastic strain ε_{xy}.

The solid line in Fig. 1 is a fit of the elastic softening in C_{66} by eq. (7) with the negative Weiss temperature $\Theta = -47.5$ K and the positive Jahn–Teller energy $\Delta = 20$ K for zero field. As we can see in Fig. 1, the softening of C_{66} in fields of 10 T shows almost the same behavior of that in zero field. The robustness of the Weiss temperature Θ in fields implies that the orbital degenerate ground state is free from magnetism in the present system. We adopt the background of $C_{66}^0 = AT + B$ with $A = -7 \times 10^5$ J/(m^3·K) and $B = 1.0735 \times 10^{10}$ J/m^3. The fitting of eq. (7) to the elastic softening in the experiments seems to be almost perfect. This result suggests that the electric quadrupole $O_{v'}$ associated with the degenerate $d_{y'z}$ and $d_{zx'}$ orbital states is relevant in the present system.

In the previous results obtained by Yoshizawa *et al.*, positive values of the Weiss temperature $\Theta = 77.5$ K for $x = 0.037$ and $\Theta = 17.2$ K for $x = 0.06$ accompanying the structural phase transitions were reported.[19] This result indicates that the doping of electrons via Co substitution for Fe leads to a reduction of the Weiss temperature Θ and changes Θ from positive at $x = 0.037$ and 0.06, indicating the ferroquadrupole ordering of the structural phase transition, to the negative sign of antiferroquadrupole interaction in the overdoped region, causing the emergence of the superconductivity with the present $x = 0.10$. This means that the quantum critical point in the proximity of the Co concentration $x_{QCP} \sim 0.07$ favors $\Theta = 0$ K of eq. (7) of C_{66}.

By using the Jahn–Teller energy $\Delta = 20$ K, the elastic constant $C_{66}^0 = 1.05 \times 10^{10}$ J·m^{-3} and the number of the Fe-ion in unit volume $D = 4.903 \times 10^{27}$ m^{-3}, we determined the quadrupole-strain coupling constant to be $g = 1760$ K/Fe-ion in eq. (2) in the present compound $Ba(Fe_{0.9}Co_{0.1})_2As_2$. This result is comparable to $g \sim 1000$ K in $(C_{11} - C_{12})/2$ in the manganese compounds of $La_{1-x}Sr_xMnO_3$ ($x = 0.12$) and $Pr_{1-x}Ca_xMnO_3$ ($x = 0.35$, 0.40, and 0.50) showing colossal magnetic resistance.[24]

In summary, the present ultrasonic experiments on the iron pnictide superconductor $Ba(Fe_{0.9}Co_{0.1})_2As_2$ revealed marked elastic softening of 21% in the shear elastic constant C_{66} down to the transition temperature $T_{SC} = 23$ K. The other shear elastic constants of $(C_{11} - C_{12})/2$ and C_{44} revealed no sign of softening around T_{SC}. Analysis based on eq. (7) showed a negative Weiss temperature $\Theta = -47.5$ K, which is in contrast to the positive Θ for the underdoped compounds with structural transitions. The softening of C_{66} decreases of 0.2% under applied magnetic fields up to 10 T at 39 K in the normal phase. The quadrupole $O_{v'}$ associated with degenerate $d_{y'z}$ and $d_{zx'}$ bands brings about the elastic softening in C_{66} and may participate in the Cooper pairing in the iron pnictide superconductivity. This result supports the theory based on Cooper pairing mediated by the orbital fluctuation favoring s_{++} symmetry.[16,17]

Acknowledgments This work was supported by a Grant-in-Aid for Specially Promoted Research (No. 18002008) "Strongly correlated quantum phases associated with charge fluctuations" from the Ministry of Education, Culture, Sports, Science and Technology of Japan. The authors are grateful to Professor H. Fukuyama, Professor B. Lüthi, Professor Y. Ōno, Dr. Y. Yanagi, and Dr. Y. Yamakawa for valuable discussions.

1) Y. Kamihara, T. Watanabe, M. Hirano, and H. Hosono: J. Am. Chem. Soc. **130** (2008) 3296.
2) J. Paglione and R. L. Greene: Nat. Phys. **6** (2010) 645.
3) Z. A. Ren, W. Lu, J. Yang, W. Yi, X. L. Shen, Z. C. Li, G. C. Che, X. L. Dong, L. L. Sun, F. Zhou, and Z. X. Zhao: Chin. Phys. Lett. **25** (2008) 2215.
4) M. Putti, I. Pallecchi, E. Bellingeri, M. R. Cimberle, M. Tropeano, C. Ferdeghini, A. Palenzona, C. Tarantini, A. Yamamoto, J. Jiang, J. Jaroszynski, F. Kametani, D. Abraimov, A. Polyanskii, J. D. Weiss, E. E. Hellstrom, A. Gurevich, D. C. Larbalestier, R. Jin, B. C. Sales, A. S. Sefat, M. A. McGuire, D. Mandrus, P. Cheng, Y. Jia, H. H. Wen, S. Lee, and C. B. Eom: Supercond. Sci. Technol. **23** (2010) 034003.
5) P. C. Canfield and S. L. Bud'ko: Annu. Rev. Condens. Matter Phys. **1** (2010) 27.
6) M. Rotter, M. Tegel, D. Johrendt, I. Schellenberg, W. Hermes, and R. Pöttgen: Phys. Rev. B **78** (2008) 020503(R).
7) Q. Huang, Y. Qiu, W. Bao, M. A. Green, J. W. Lynn, Y. C. Gasparovic, T. Wu, G. Wu, and X. H. Chen: Phys. Rev. Lett. **101** (2008) 257003.
8) S. Nandi, M. G. Kim, A. Kreyssig, R. M. Fernandes, D. K. Pratt, A. Thaler, N. Ni, S. L. Bud'ko, P. C. Canfield, J. Schmalian, R. J. McQueeney, and A. I. Goldman: Phys. Rev. Lett. **104** (2010) 057006.
9) I. A. Nekrasov, Z. V. Pchelkina, and M. V. Sadovskii: JETP Lett. **88** (2008) 144.
10) F. Ning, K. Ahilan, T. Imai, A. S. Sefat, R. Jin, M. A. McGuire, B. C. Sales, and D. Mandrus: J. Phys. Soc. Jpn. **78** (2009) 013711.
11) H. Ding, P. Richard, K. Nakayama, K. Sugawara, T. Arakane, Y. Sekiba, A. Takayama, S. Souma, T. Sato, T. Takahashi, Z. Wang, X. Dai, Z. Fang, G. F. Chen, J. L. Luo, and N. L. Wang: Europhys. Lett. **83** (2008) 47001.
12) I. I. Mazin and J. Schmalian: Physica C **469** (2009) 614.
13) K. Kuroki, S. Onari, R. Arita, H. Usui, Y. Tanaka, H. Kontani, and H. Aoki: Phys. Rev. Lett. **101** (2008) 087004.
14) M. Sato, Y. Kobayashi, S. C. Lee, H. Takahashi, E. Satomi, and Y. Miura: J. Phys. Soc. Jpn. **79** (2010) 014710.
15) S. C. Lee, E. Satomi, Y. Kobayashi, and M. Sato: J. Phys. Soc. Jpn. **79** (2010) 023702.
16) Y. Yanagi, Y. Yamakawa, N. Adachi, and Y. Ōno: J. Phys. Soc. Jpn. **79** (2010) 123707.
17) H. Kontani and S. Onari: Phys. Rev. Lett. **104** (2010) 157001.
18) R. M. Fernandes, L. H. VanBebber, S. Bhattacharya, P. Chandra, V. Keppens, D. Mandrus, M. A. McGuire, B. C. Sales, A. S. Sefat, and J. Schmalian: Phys. Rev. Lett. **105** (2010) 157003.
19) M. Yoshizawa, R. Kamiya, R. Onodera, Y. Nakanishi, K. Kihou, H. Eisaki, and C. H. Lee: arXiv:1008.1479.
20) A. S. Sefat, R. Jin, M. A. McGuire, B. C. Sales, D. J. Singh, and D. Mandrus: Phys. Rev. Lett. **101** (2008) 117004.
21) B. Lüthi: in *Physical Acoustics in the Solid State*, ed. M. Cardona, P. Fulde, K. von Klitzing, and H. J. Queisser (Springer, Berlin, 2005).
22) M. Niksch, B. Lüthi, and J. Kübler: Z. Phys. B **68** (1987) 291.
23) S. Nakamura, T. Goto, M. Kasaya, and S. Kunii: J. Phys. Soc. Jpn. **60** (1991) 4311.
24) H. Hazama, T. Goto, Y. Nemoto, Y. Tomioka, A. Asamitsu, and Y. Tokura: Phys. Rev. B **62** (2000) 15012; H. Hazama, T. Goto, Y. Nemoto, Y. Tomioka, A. Asamitsu, and Y. Tokura: Phys. Rev. B **69** (2004) 064406.